The College of Engineering
University of Wisconsin-Madison

Wisconsin Electric Machines and Power Electronics Consortium

RESEARCH REPORT
87-24

DESIGN OF A ROBUST CONTROLLER FOR DIRECT FIELD ORIENTED CONTROL OF AN INDUCTION MOTOR

F. Profumo, D. Zinger and T.A. Lipo
Dept. of Electrical and Computer Engr.
University of Wisconsin-Madison
1415 Johnson Drive
Madison, WI 53706-1691

WEMPEC

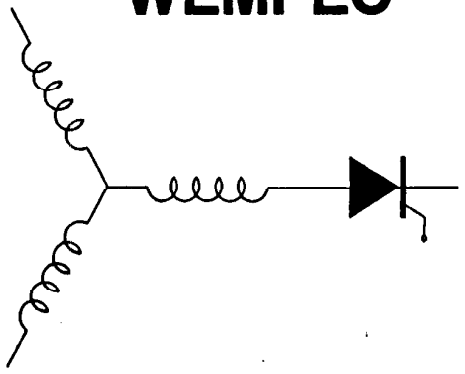

Department of Electrical and Computer Engineering
1415 Johnson Drive
Madison, Wisconsin 53706
June 1987

DESIGN OF A ROBUST CONTROLLER FOR DIRECT FIELD ORIENTED CONTROL OF AN INDUCTION MOTOR

F. Profumo, D. Zinger and T A. Lipo
University of Wisconsin
Department of Electrical and Computer Engineering
1415 Johnson Drive
Madison, Wisconsin, 53706, U.S.A.

Abstract Present-day field oriented controllers utilize a shaft encoder to achieve orientation of the rotor flux to stator current. However, the cost of such systems is relatively high. Also, the algorithm is prone to errors due to incorrect gain setting and/or time changing parmeters. This paper presents a new robust controller which utilizes the windings of the machine itself to implement field orientation. As a result the system does not require shaft speed or position sensing. A new flux regulator is discussed which utilizes PD rather than the traditional PI regulator. Confirmation of the theory is demonstrated with experimental results.

INTRODUCTION

Traditional open loop adjustable speed drives today cover a large number of industrial applications in which the precise speed regulation and fast torque are not required. On the other hand, sophisticated closed loop solutions with a complete indirect or direct field oriented controller are used to obtain outstanding high performance in terms of speed and torque response. The price to pay for the latter solution is a more complex hardware implementation which needs also an expensive position encoder and/or special flux sensors.

It appears that the increasing popularity of the field oriented control technique [1] is limited by the cost level , which, while acceptable for servo-type applications, is excessive when compared to the open loop controllers serving the bulk of the ac drive market. From this point of view a desirable goal appears to be the development of a motor drive without tachometer or other position encoder for speed detection and a motor without search coils or Hall effect coils for flux sensing and reducing to a minimum the sensors used for control purposes. However, this requirement is not well suited to the traditional approach employing the indirect vector control scheme. In addition to the need for a position/speed sensor, this control method uses a model of the machine to calculate the rotor flux angle. The approach is unfortunately also sensitive to the values of the machine parameters which can vary with the temperature and/or the magnetic saturation level and it needs sophisticated algorithms for compensating the above mentioned non ideal behavior.

The goals of the research reported in this paper has been to design a drive with a large speed operation range (3 Hz to the maximum frequency available, as required by the industrial application), with the simplest possible structure for all the drive components including motor, power electronics structure and control and with a large insensitivity to the machine parameters over a wide range of operating conditions [2,3]. The solution presented in this paper is a direct field oriented controller without tachometer having tapped stator windings for flux sensing [4,5]. The overall information available from the voltage detected is utilized for a proportional-derivative (PD) flux loop control and for the speed loop without introducing additional analog or digital derivative calculators.

FLUX SENSING PRINCIPLE

In order to eliminate the need for added flux sensors a method has been previously developed to measure the flux by using the induced voltage of at least two coils in each phase. The induced voltage is measured by taps that have been attached to the coils themselves [5]. This approach can be implemented in a a straightforward manner by simply making additional connections at the ends of the selected stator coils.

In Fig. 1a two simplified identical stator coils used as flux sensors are shown and in Fig. 1b their equivalent circuit is depicted where L is the self and mutual inductance and r is the resistance of the coil. Reference describes in more detail this method for measuring air gap flux which

utilizes two coils for each phase of the motor itself.

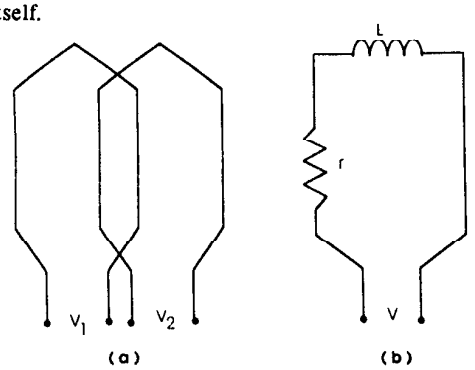

Fig. 1: a) Pictorial diagram of 2 overlapping coils in same phase. b) Equivalent schematic for coil.

This scheme is not affected by temperature nor by the *ir* drop in the motor coils and therefore remains a reliable measurement even when the ohmic drop is relatively large and time varying. In particular the d - component of the air gap flux λ_{dm} is proportional to:

$$\lambda_{dm} = k_1[\int (v_{a_1} - v_{a_2})dt] \quad (1)$$

and the q - component λ_{qm} can be expressed by:

$$\lambda_{qm} = k_2 \left[\int (v_{b_1} - v_{b_2})dt - \int (v_{c_1} - v_{c_2}) \right]dt \quad (2)$$

where a_1 and a_2 are the coils related to phase a, b_1 and b_2 to phase b and c_1 and c_2 to phase c.

Finally the air gap flux λ_m can be written in the following way:

$$\lambda_m = \sqrt{\lambda_{dm}^2 + \lambda_{qm}^2} \quad (3)$$

DIRECT FIELD ORIENTATION PRINCIPLE

A) Flux Loop Control

It is well known that the direct flux sensing method typically senses the derivative components of the air gap flux whereas the variable to be controlled is the rotor flux. The equations which defines the relationships between the air gap flux, rotor flux and stator current are expressed by:

$$\lambda_{dr}^s = \frac{L_r}{L_m}\lambda_{dm}^s - L_{r\sigma} i_{ds}^s \quad (4)$$

$$\lambda_{qr}^s = \frac{L_r}{L_m}\lambda_{qm}^s - L_{r\sigma} i_{qs}^s \quad (5)$$

where λ_{dr}^s and λ_{qr}^s are the components of the rotor flux desired, L_r is the rotor self inductance, L_m is the mutual inductance, λ_{dm}^s and λ_{qm}^s are the components of the air gap flux, $L_{r\sigma}$ is the rotor leakage and i_{ds}^s and i_{qs}^s are the components of the stator current. The superscript s represents the stationary reference frame.

This approach has the appreciable advantage of requiring knowledge of only two motor parameters, the rotor leakage inductance $L_{r\sigma}$ (which is almost constant independent of temperature or flux level) and the ratio self inductance to mutual inductance L_r/L_m which is only moderately affected by saturation in the machine. The scheme requires two CTs for the stator current detection. A simplified diagram of the flux loop control is depicted in Fig. 2 wherein λ_r^* is the reference flux, K_P is the proportional gain of PI controller and i_{ds}^* is the stator current component for the flux command.

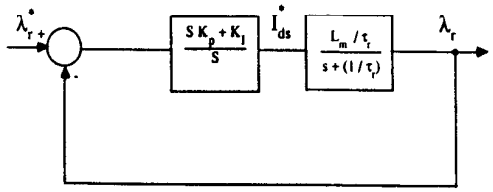

Fig. 2: Simplified flux control loop with PI controller.

As a first observation it can be noted that with this control loop we have pair of poles that causes delays and sluggish response. If we represent the motor in simplified maner using only the rotor time constant $\tau_r = L_r/r_r$, then the open loop locus roots are depicted in Fig. 3.

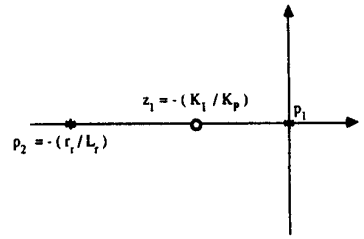

Fig. 3: Open loop pole-zero placement for flux loop with PI controller.

The basic strategy for this regulator is to set the zero of the system at such a point that with sufficient gain, the integrator pole of the PI controller is near the zero, and also the rotor time constant pole has moved sufficiently far to left in the root plane that its time constant becomes

neglible. Although this system is stable, it can often be sluggish since substantial gain often cannot be introduced into the transfer function without introducing non-linear behavior.

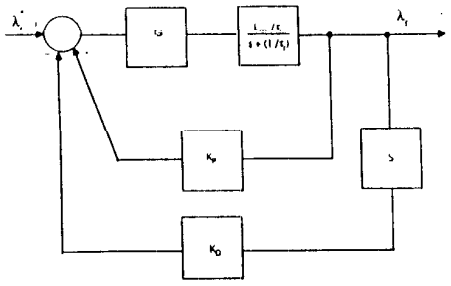

Fig. 4: Simplified flux control loop with PD feedback control.

Utilizing the system implemented with flux sensing we have, in effect, two state variables available ($\frac{d\lambda}{dt}$ and λ), and it would be useful to design a new flux controller with faster response time by making use of this added information. A suitable control loop to satisfy this requirement is shown in Fig. 4. In practice only the derivative component of the air gap flux is directly available and it is necessary to regenerate the rotor flux. However, starting from the Eqs (4) and (5) , and differentiating the left and right side, we have:

$$\frac{d\lambda_{dr}^{s}}{dt} = \left(\frac{L_r}{L_m}\right)\frac{d\lambda_{dm}^{s}}{dt} - L_{r\sigma}\frac{di_{ds}^{s}}{dt} \qquad (6)$$

$$\frac{d\lambda_{qr}^{s}}{dt} = \left(\frac{L_r}{L_m}\right)\frac{d\lambda_{qm}^{s}}{dt} - L_{r\sigma}\frac{di_{qs}^{s}}{dt} \qquad (7)$$

where $\frac{di_{ds}^{s}}{dt}$ and $\frac{di_{qs}^{s}}{dt}$ are not at present available.

It is apparent that, to calculate the derivative components of rotor flux. an analog or digital sensor will be needed for differentiating the stator current. In Appendix A is presented a simple and low cost solution utilizing a signal.

Finally, it is not difficult to deduce the expression for the magnitude of the derivative component of the rotor flux:

$$|\lambda_r| = \sqrt{\lambda_{dr}^2 + \lambda_{qr}^2} \qquad (8)$$

$$\left|\frac{d\lambda_r}{dt}\right| = \frac{\lambda_{dr}\frac{d\lambda_{dr}}{dt} + \lambda_{qr}\frac{d\lambda_{qr}}{dt}}{\sqrt{\lambda_{dr}^2 + \lambda_{qr}^2}} \qquad (9)$$

In Fig. 5 shown below there is the complete scheme of the new rotor flux loop controller.

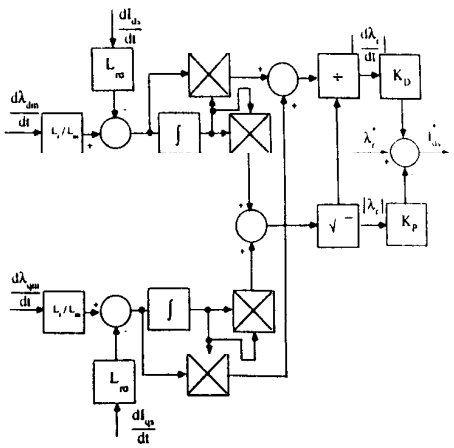

Fig. 5: Detailed diagram of flux control loop with PD feedback control.

As is well known, the field orientation technique requires that the current commands must be oriented to the rotor flux (Fig. 6a) and errors in orientation may cause an improper flux setting (Fig. 6b).

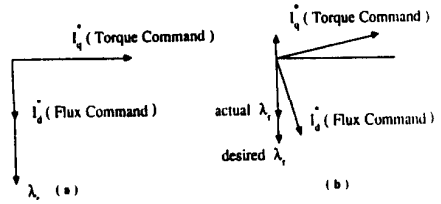

Fig. 6: Relationship of field oriented current command vectors to flux vector for : a) properly oriented command. b) improperly oriented commands.

However, fast action of the flux regulator can compensate for such errors and the aim of the new flux regulator is to improve the time response of the flux changes. Starting from the simplified diagram (Fig. 7), the system can be studied in a straightforward manner and the controller can be designed with any desirable position for the zero $z_1 = -\frac{K_P}{K_D}$ for improving the system performances without stability problems. In Fig. 8 the open loop roots are shown.

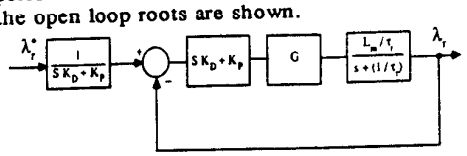

Fig. 7: Simplified flux control loop placing the PD controller in feedforward path.

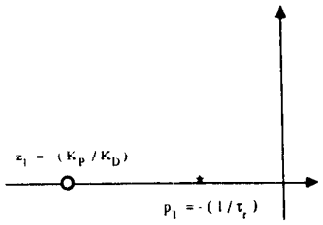

Fig. 8: Open loop pole zero placement for PD feedback controller.

B) Speed Loop

Because our goal is to design a low cost drive without giving up the good performance of a field oriented controller, the removal of the tachometer and any other position sensor is mandatory. However the design of the speed loop requires a signal proportional to the actual mechanical speed or at least to the rotor flux frequency disregarding the slip compensation. In order to calculate this frequency, the simplest method is to follow Eq. 9, starting from the derivative component of rotor flux and from the rotor flux following the procedure depicted in Fig. 9. An output filter with a cut off frequency fixed at 5 Hz is necessary for decreasing the noise coming from the input signal. The actual range of operation of such a frequency estimator is quite large: working from 3 Hz to up to the maximum operation frequency.

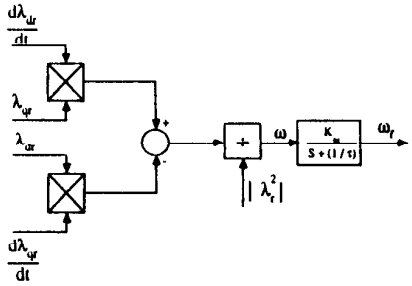

Fig. 9: Method used to determine synchronous frequency.

IMPLEMENTED SOLUTION

On the basis of the considerations above, a drive system with the desired characteristics has been implemented in our laboratory. A three phase induction motor with tapped stator windings has been utilized supplied by a current controlled PWM inverter that utilizes power transistors as its power switching devices. The output voltage of the inverter is only 120 V and being the motor 230 V rated voltage the maximum speed is about 900 rpm (30 Hz). In Appendix B the main characteristics of the motor are listed.

A pulse width wave form is generated from the difference between the current command and the actual wave form using a ramp comparator and the computation of the current command from the flux voltages and the line derivative currents using the direct field oriented control method has been implemented in digital manner by a microprocessor Intel 80286.

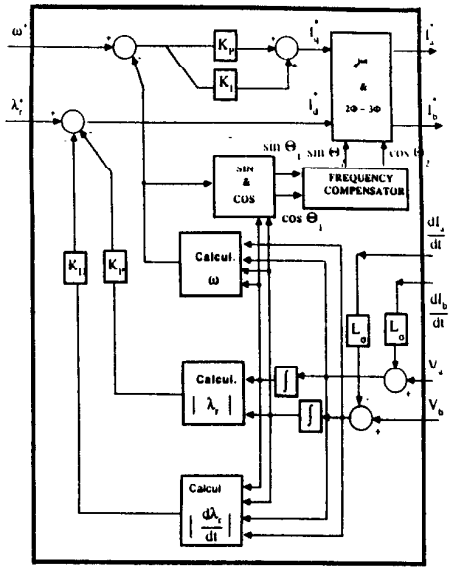

Fig. 10: Overall control system.

Figure 10 shows a simplified block diagram of the system implementation and shows some details about the control functions. The interface between the analog world (flux voltages and derivative of current) and the digital world is realized by operations of A/D conversion that are the first step inside the process of calculation of all the functions in the field orientation control algorithm. In order to achieve a good control over the system, the total execution time for the motor functions as rotor flux calculation, sine and cosine calculations, frequency detection, proportional-plus-derivative (PD) controller for the flux loop, proportional-plus-integral (PI) controller for the speed loop and phase and reference frame transformation must be as short as possible. However, all these operations have to be executed at exact time intervals. To accomplish this task the software is structured in the 'initialization program' (one time executed) and the various por-

tions such as major control parameter settings (and updating by keyboard), interrupt controller setting and A/D and D/A converter initialization are carried out. In the 'user interface program' which runs in the time between the end of one interrupt and start of the next interrupt and its function is to allow the user control and update over the speed and termination of the program through the keyboard. The "user program" is started when each interrupt is executed and accomplishes all the major functions of the field orientations control algorithm (the heart of the control). The interrupt time is set at 1 millisecond. The interface between the digital and analog world is realized through a D/A conversion that outputs the current command to the inverter completing the field control task.

EXPERIMENTAL RESULTS

With reference to the previous discussion. three different cases have been chosen for testing the new controller in our laboratory. The selected case number one is the "PD feed back" flux controller in which we endeavored to optimize the two constants K_P for the proportional path and K_D for the derivative one. The selected case number 2 is an "open loop drive" derived from the previous case, but setting K_P and K_D to zero. Finally the selected case number 3 is a "traditional PI flux controller" using the double integration: the first integrator to calculate the flux starting from the derivative component of flux and the second inside the PI controller itself.

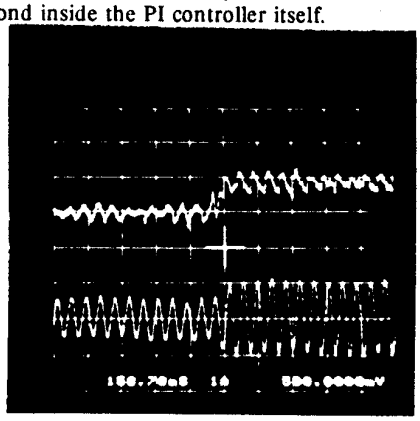

Fig. 11: Flux response for a step change in flux command for PD feedback controller. Top: Magnitude of flux. Bottom: Phase A rotor flux waveform. Time scale: 0.15 S/div.

The comparison among the different cases take place from the flux step command and from the speed step change; both in no load conditions. In Fig. 11 the magnitude of rotor flux and the actual flux are shown related to the case number 1 for a step in the flux command. . The rise time is about 50 msec and K_P and K_D are large enough to allow setting of the closed loop pole of the control system dependent only on the $\frac{K_P}{K_D}$ ratio and independent of the actual rotor time constant of the machine. This result is clearly desirable since the controller setting is straightforward and independent from the machine parameters.

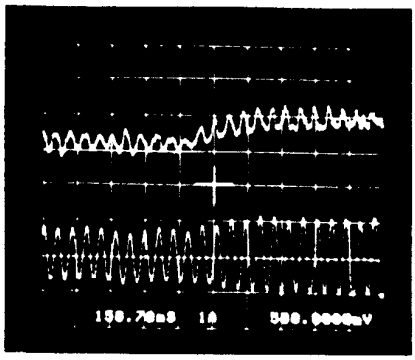

Fig. 12: Flux response to a step change in flux command for an open loop control. Top: Magnitude of flux. Bottom: Phase A rotor flux waveform. Time scale: 0.15 S/div.

In Fig. 12, the magnitude of rotor flux and the actual flux for a step in the flux command are depicted for the open loop case in which the rise time is strictly related to the rotor time constant of the machine. The rise time is about 250 msec in this case. Finally Fig. 13 shows the same wave forms related to the normal PI controller. A rise time of about 180 msec can be noted.

The second series of tests correspond to a step speed change decrease and increase. The speed and the actual flux are depicted for each case.

In Figs. 14, 15, and 16 related to the cases 1-3 respectively, the speed is changed from 900 rpm (30 Hz) down to 120 rpm (4 Hz). In Figs. 17-19 the speed step is instead changed from 120 rpm (4 Hz) up to 900 rpm (30 Hz).

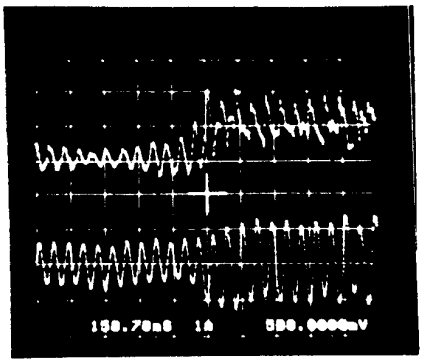

Fig. 13: Flux response for a step change in flux command for a PI control. Top: Magnitude of flux. Bottom: Phase A rotor flux waveform. Time scale: 0.15 S/div.

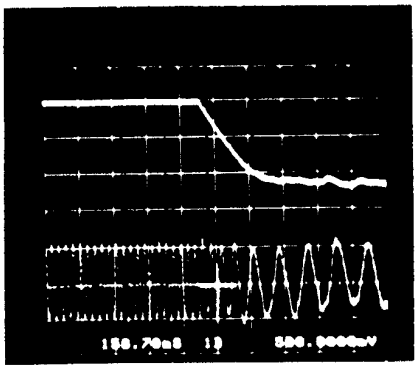

Fig 14: Response to a step in speed command from 900 rpm to 120 rpfm with PD feedback in flux loop. Top trace: Speed. Bottom trace: Phase A rotor flux waveform. Time scale: 0.15 S/div.

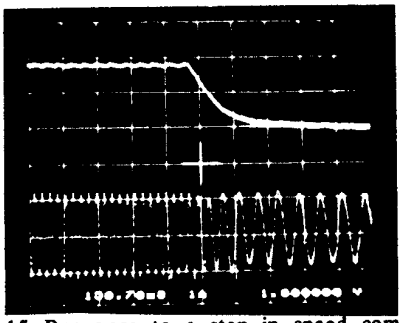

Fig. 15: Response to a step in speed command from 900 rpm to 120 rpm with an open loop flux control. Top trace: Speed. Bottom trace: Phase A rotor flux waveform. Time scale 0.15 S/div.

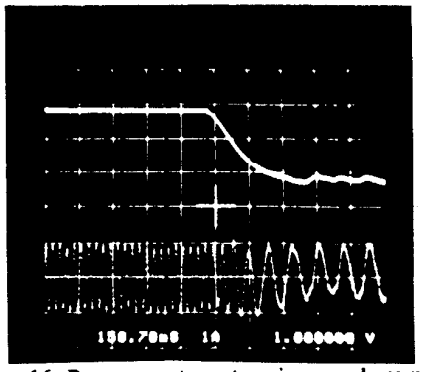

Fig. 16: Response to step in speed command from 900 rpm to 120 rpm with PI controller in flux loop. Top trace: Speed. Bottom trace: Phase A rotor flux waveform. Time scale 0.15 S/div.

As it is possible to note from the pictures the times rise for the step increase and decrease are generally consistent and depend primarily on the speed loop controller which, for each case, is set with the same values.

CONCLUSION

A solution for a low cost direct field orientated drive has been presented. The approach is attractive due to its hardware and software simplicity and good performance in comparison to the PI controller drive. The major advantages are due to the straightforward design for the flux loop controller starting from the available state variables of the tapped stator winding machines: the air gap flux and the derivative of air gap flux. The wide speed range of operation of the machine from 4 Hz to 30 Hz (the upper limit is related to the output voltage of the inverter 120 V for driving a machine rated 230 Volts) makes this solution attractive to a large number of industrial applications in which a motor drive having good performance without position or speed sensor required.

ACKNOWLEDGMENTS

The work of the authors reported in this paper was made possible by support from the industrial sponsors of the Wisconsin Electric Machines and Power Electronics Consortium (WEMPEC) to whom the authors are greatly indebted.

REFERENCES

[1] V. R. Stefanovic, *"Present Trends in Variable Speed AC Drives"*, Proc. of International Power Electronics Conference, Mar 27-31 1983, pp. 438-449.

[2] K. Nordin, D. W. Novotny, and D. S. Zinger, *"The Influence of Motor Parameter Deviations in Feedforward Field Oriented Drive Systems"*, IEEE Transactions on Industry Applications, July/Aug 1985, pp.1009-1015.

[3] R. D. Lorenz, *"Tuning of Field-Oriented Induction Motor Controllers for High Performance Applications"*, IEEE Trans. on Industry Applications, vol 1A-22, No. 2, March/April 1986, pp. 293-297.

[4] F. Benzi, D. Zinger, and T. A. Lipo, *"A New Approach to Induction Motor Torque and Speed Control"*, Proc. of Conference on Applied Motion Control '86, Minneapolis, MN, June 10-12, 1986, pp.25-29.

[5] T. A. Lipo and K. C. Chang, *"A New Approach to Flux and Torque Sensing in Induction Machines"*, in Conf. Rec. IEEE IAS Annual Meeting, Oct 1985, pp. 765-769.

APPENDIX A

The choice of the tool for finding the derivative of the two stator currents was a challenging task. In an intitial stage it was decided to use traditional analog or digital derivative calculators using two CTs for current sensing. As well known, such an approach increases the noise and the initial results were very poor. On the other hand our goal was to design a low cost drive and the following idea seemed close enough to our aims: reliability, low price and wide band width.

The best, and ultimately the simplest solution was to place a suitable number of turns in parallel to the motor main wire supply as shown in Fig. A.1.

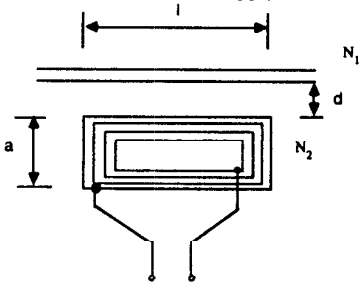

Fig. B.1:Diagram of arrangement used to measure current derivative.

The voltage $v(t)$ results:

$$v(t) = M\frac{di}{dt} = \mu_0\frac{lN_2N_1}{2\pi}\ln\left(\frac{a+d}{d}\right)\frac{di}{dt} \qquad (A.1)$$

where the symbols are self explained in the figure. The output voltage is clearly proportional to the time derivative of the current as desired. The total cost is only about US$ 10.00.

To obtain a reasonable output voltage, it was necessary to amplify the output signal by a factor of 100. Finally, it was necessary to determine the correct value of M for using the correct $\frac{di}{dt}$ in our control. A simple integration of $v_1(t)$ was used for this purpose and the result compared with the normal CT output. It is interesting to mention that the integrated current waveform was essentially identical to the much more expensive Hall Effect current sensor.

Finally, only a few words about the name of this rather unique transformer. The support for the N_2 turns has been realized with a simple wooden block. To the casual visitor to our lab, our "wood transformer" was a bit of "black magic" which we happily displayed and enjoyed immensely.

APPENDIX B- MACHINE PARAMETERS

Rated Power = 10 *Hp*
Rated Voltage = 230 *V*
Rated Frequency = 60 *Hz*
Poles = 4
Rated Speed = 1800*RPM*
R_s = 0.0624Ω
$X_{s\sigma}$ = 0.185Ω
R_r = 0.0312Ω
$X_{r\sigma}$ = 0.183Ω
X_m = 2.3107Ω